The Journal of Veterinary Medical Science

FULL PAPER

Anatomy

# Three-dimensional analysis of neural connectivity with cells in rat ileal mucosa by serial block-face scanning electron microscopy

**Satoki NAKANISHI[1)], Youhei MANTANI[1)]*, Tomohiro HARUTA[3)], Toshifumi YOKOYAMA[2)] and Nobuhiko HOSHI[2)]**

[1)]Laboratory of Histophysiology, Department of Bioresource Science, Graduate School of Agricultural Science, Kobe University, 1-1 Rokkodai-cho, Nada-ku, Kobe, Hyogo 657-8501, Japan

[2)]Laboratory of Animal Molecular Morphology, Department of Bioresource Science, Graduate School of Agricultural Science, Kobe University, 1-1 Rokkodai-cho, Nada-ku, Kobe, Hyogo 657-8501, Japan

[3)]Bio 3D Promotion Group, Application Management Department, JEOL Ltd., 3-1-2, Musashino, Akishima, Tokyo 196-8558, Japan

**ABSTRACT.** The comprehensive targets of innervation in the intestinal mucosa are unknown, partly because of the diversity of cell types and the complexity of the neural circuits. Herein, we investigated the comprehensive targets of neural connectivity and analyzed the precise characteristics of their contact structures in the mucosa of rat ileum. We examined target cells of neural connections and the characteristics of their contact structures by serial block-face scanning electron microscopy at four portions of the rat ileal mucosa: the apical and basal portions in the villi, and the lateral and basal portions around/in the crypts. Nerve fibers were in contact with several types of fibroblast-like cells (FBLCs), macrophage-like cells, eosinophils, lymphocyte-like cells, and other types of cells. The nerve fibers almost always ran more inside of lamina propria than subepithelial FBLC, and thus contacts with epithelial cells were very scarce. The contact structures of the nerve fibers were usually contained synaptic vesicle-like structures, and we classified them into patterns based on the number of nerve fiber contacting the target cells at one site, the maximum diameter of the contact structures, and the relationship between nerve fibers and nerve bundles. The contact structures for each type of cells occasionally dug into the cellular bodies of the target cells. We revealed the comprehensive targets of neural connectivity based on the characteristics of contact structures, and identified FBLCs, immunocompetent cells, and eosinophils as the candidate targets for innervation in the rat ileal mucosa.

**KEY WORDS:** electron microscopy, enteric nervous system, nerve fiber, rat, small intestine

*J. Vet. Med. Sci.*
82(7): 990–999, 2020
doi: 10.1292/jvms.20-0175

Received: 27 March 2020
Accepted: 7 May 2020
Advanced Epub: 2 June 2020

The enteric nervous system (ENS) regulates fundamental functions in the intestine including blood flow, motility, and the secretion of intestinal juices [11]. Neurons in the guinea pig, mouse, and pig ENS have been reported to comprise various subtypes that possess a variety of neurotransmitters including vasoactive intestinal peptide (VIP), acetylcholine (ACh), neuropeptide Y, and substance P (SP) [11, 34, 39]. The effects of these neurotransmitters on the gastrointestinal tract and each type of tissue or cells in the intestine have been investigated. For example, VIP was reported to induce the relaxation of smooth muscle [33] and vasodilation [18] in the rat stomach. ACh may contract the longitudinal and circular muscles in the large intestine of rabbits [15], expand blood vessels in the intestine of guinea pigs [30], and induce the secretion of antibacterial substances from Paneth cells in the rat small intestine [35]. SP and calcitonin gene-related peptide (CGRP) facilitate the proliferation of epithelial cells in the rat colon [17]. The function of each neurotransmitter is thus gradually becoming clear, but little is known about the "big picture" of the target for innervation in the intestinal mucosa, because the cellular composition is highly complicated at that site.

The innervation in the mucosa is speculated to be able to occur by paracrine manner without direct contact, because the neurotransmitter from autonomic nerves have been considered to diffuse for distances [21]. However, transmission electron microscopy (TEM) has revealed that the innervation by direct contact could occur against subepithelial and non-subepithelial fibroblast-like cells (FBLCs) [9, 16, 29], mononuclear phagocytes [4], and mast cells [38] in the intestinal mucosa. These ultrastructural observations by TEM have contributed to evaluations of the existence of potential innervation with direct contact, but it is difficult to comprehensively trace the nerve fibers that resemble a mesh, even with TEM. It is also a challenge to determine the exact manner of neural connections, which is speculated to be varicosity-like [21]. In the present study, we used serial

*Correspondence to: Mantani, Y.: mantani@sapphire.kobe-u.ac.jp

block-face scanning electron microscopy (SBF-SEM), which is one of the technologies for serial ultrastructural observation using electron microscopy, gathering attention in the brain connectome [32]. With SBF-SEM, any tissue structures can be analyzed at nanometer-order and in a three-dimensional (3D) format [8]. A 3D analysis obtained by SBF-SEM enables investigators to not only trace nerve fibers but also obtain the detailed morphological characteristics of innervated cells over a wide area.

Our earlier study revealed that the rat ileal lamina propria contains four morphologically distinct types of FBLCs, macrophage-like cells (MLCs), lymphocyte-like cells, eosinophils, plasma cells, and other cells [25], and these findings provided useful information for evaluations of the connective targets of the nerve fibers in the intestinal mucosa. Here, we focused on the innervation by direct contact and comprehensively evaluated the connectivity of nerve fibers running in the lamina propria for each type of cells in the rat ileum. We also sought to determine the precise characteristics of contact structures that have been suspected to be varicosities and discuss the presence of the innervation with direct contact for each type of cells in the rat ileal mucosa.

## MATERIALS AND METHODS

In this study, we reused the data stacks obtained by SBF-SEM in our earlier study [25]; therefore, animals, tissue blocks and data stacks are the same as our earlier study [25].

### *Animals*

Six 7-week-old male Wistar rats (Japan SLC, Hamamatsu, Japan) were maintained under specific pathogen-free conditions in individual ventilated cages (Sealsafe Plus; Tecniplast, Bugugiate, Italy). They were permitted free access to water and food (Lab RA-2; Nosan Corp., Yokohama, Japan). The animal facility was maintained under a 12-hr/12-hr light/dark cycle at 23 ± 2°C and 50 ± 10% humidity. Clinical and pathological examinations in all animals confirmed that there were no signs of disorder. This animal study was approved by the Institutional Animal Care and Use Committee (Permission no. 25-06-01) and carried out according to the Kobe University Animal Experimentation Regulations.

### *Acquisition of data stacks with SBF-SEM and 3D reconstruction of histological components*

For this investigation, we reused the data stacks obtained in our earlier investigation [25] for the 3D reconstruction of nerve fibers and nerve bundles. Briefly, ileal blocks from six rats were fixed with 2.5% glutaraldehyde and 2.0% paraformaldehyde fixative in 0.1 M cacodylate buffer (CB; pH 7.4) and postfixed with 2.0% $OsO_4$/1.5% potassium ferrocyanide in CB. All specimens were washed in distilled water, incubated with 1.0% thiocarbohydrazide, postfixed with 2.0% $OsO_4$ stained with 4.0% uranyl acetate overnight and with 0.4% aspartic acid/0.66% lead nitrate, and then dehydrated and embedded in an Epon 812 mixture. Ketjen black was added to a resin mixture, which was then used to embed a part of the sample for the observations of the intestinal villus. The Ketjen black, which is useful to prevent charging of the samples [31], was kindly provided by Dr. N. Ohno. We used a JSM 7800F SBF-SEM system (JEOL, Tokyo, Japan) with a Gatan 3View 2XP system (Gatan, Abingdon, UK) to obtain data stacks from the following four portions of the rat ileal mucosa: the apical portion of the villi (IVA), the basal portion of the villi (IVB), the lateral portion of the crypts (ICL), and the basal portion of the crypts (ICB) (Fig. 1A).

Each data stack containing ≥450 images was obtained with a 100 nm slice pitch for observations of the broad area of ileal mucosa and then aligned using Fiji or DigitalMicrograph software (Gatan). Nerve fibers, contacting with any of the types of cells in the lamina propria, and nerve bundles including enteric glial cells were three-dimensionally reconstructed from these aligned data stacks with the use of the program IMOD (https://bio3d.colorado.edu/imod/).

### *Tentative classification of cells in the lamina propria for the analysis of neural connectivity*

To analyze the connectivity of nerve fibers to each type of cell, the cells in the rat ileal lamina propria were tentatively classified based on their morphological characteristics as follows. Enteric glial cells, villous myocytes, plasma cells, eosinophils, and mast cells were easily identified, whereas several other types of cells in the lamina propria needed to be defined specifically as follows. Cells other than pericytes, vascular endothelial cells, and lymphatic endothelial cells in the lamina propria could be divided into two types by their external appearance: cells with highly irregular shapes and cells with simple shapes (sphere or oval). Irregularly shaped cells that had one or more long cellular processes were classified as FBLCs and MLCs: FBLCs, which had been already defined and identified in our earlier study [25], possessed abundant and expanded endoplasmic reticula and consisted of four types, whereas MLCs were characterized by both the existence of lysosomes and/or phagosomes and a lesser expansion of endoplasmic reticula compared to FBLCs (*unpublished data*).

In a previous study, we had already classified FBLCs in the data stacks used in the present study into four types based on the external cellular appearance, the abundance or shape of each organelle, the detailed distribution, and relationship with surrounding cells (Fig. 1B) [25]. Briefly, the type I and type II FBLCs were localized in the subepithelial region around the intestinal crypts, whereas the type III FBLCs were located in the subepithelial region, closer than the type I and II FBLCs, from the ICL to the villous apex. The type IV FBLCs were located away from the epithelium from the IVB to the IVA. The type I FBLCs contained a spherically expanded endoplasmic reticulum with a spherical shape, whereas the type II FBLCs each had a thin and multi-layered endoplasmic reticulum. The MLCs were composed of several types including typical macrophage-like cells with frequent phagosomes, the peculiar types of macrophage-like cells with abundant exoplasm reported by Iwanaga *et al*. (1994) [20], and others. We classified the cells with simple shapes (other than the plasma cells, eosinophils, and mast cells) as lymphocyte-like cells and monocyte-like cells: the lymphocyte-like cells had a spherical or oval-shaped nucleus, and the monocyte-like cells had a reniform or horseshoe-shaped

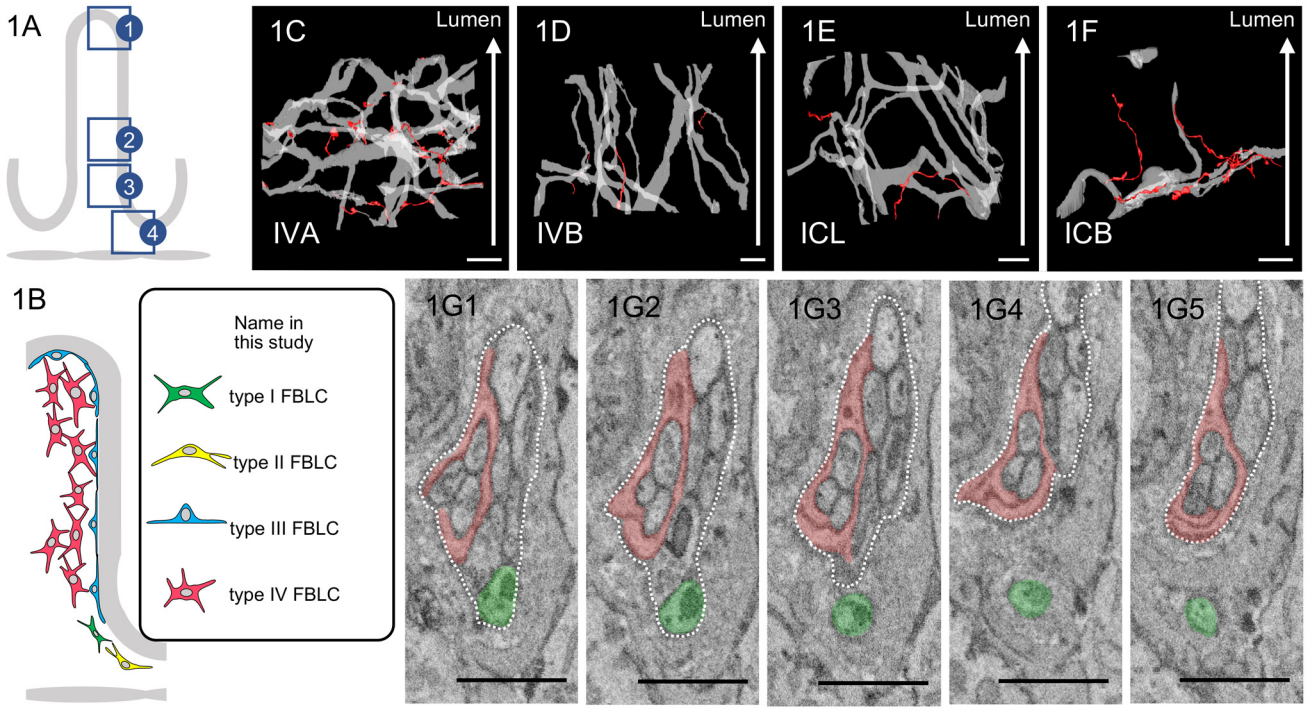


**Fig. 1.** A: Schema of observed portions of the ileal mucosa: (1) the apical portion of the villi (IVA), (2) the basal portion of the villi (IVB), (3) the lateral portion of the crypts (ICL), and (4) the basal portion of the crypts (ICB). B: Schema of classification of fibroblast-like cells (FBLCs). C–F: 3D images of the running pattern of nerve bundles, including enteric glial cells, and nerve fibers. Upper parts of images are the luminal side of the intestine (*white arrow*). Nerve bundles (*light gray*) frequently branch in the IVA (C) and ICL (E) and exhibit a greater degree of branching in the IVA compared to the IVB (D) and ICB (F). Nerve fibers (*red*) separated from the nerve bundle are more common in IVA (C) compared to the other portions. G: Serial images of a nerve fiber (*green*) separated from a nerve bundle (contoured by *white dashed line*) in IVA. Enteric glial cell (*red*) is observed as a part of the nerve bundle. C–F: Bar=10 $\mu$m. G: Bar=1 $\mu$m.

nucleus. The mucosal epithelial cells were classified into columnar epithelial cells, goblet cells, Paneth cells, and endocrine cells.

The cell type of some cells could not be identified because their cellular bodies were not sufficiently present in the data stacks; we thus refer to these cells as "undetermined cells" herein. In addition to pericytes, vascular endothelial cells, and lymphatic endothelial cells, although undefined cells other than the cells defined above were observed as minor populations in the lamina propria, their characteristics are not described herein because they had no contact with nerve fibers. Conversely, we excluded enteric glial cells from the analysis object because enteric glial cells constantly enwrapped the nerve fibers, so their contact numbers were countless.

### *Quantitative histological analysis*

The numbers of all cells that were in contact with one or more nerve fibers, including undetermined cells, were counted. We then conducted a 3D examination of all contact structures and classified them based on the number of nerve fibers contacting the target cells at one site, their relationship with nerve bundles, and the maximum diameter of each nerve fiber as described below. We also counted the number of each pattern of contact structures contacting with each type of cells in the mucosa. These results are presented as numerical data. The maximum diameter of each nerve fiber at the detected contact structure was measured from the three-dimensionally reconstructed contact structure by the Fiji program, and these data are presented as a bar chart.

## RESULTS

### *3D analysis of the neural network in the rat ileal mucosa*

Nerve bundles, including enteric glial cells, formed complex networks by branching/anastomosing with higher complexity in the IVA compared to the three other portions of the rat ileal mucosa (Fig. 1C–F). The degree of branching/anastomosis of nerve bundles was largest in the IVA and larger in the ICL than in the IVB and ICB (Fig. 1C–F). The nerve bundles in the IVB simply ran along the long axis of intestinal villi (Fig. 1D). Separation of a nerve fiber from the nerve bundle was observed in all four ileal mucosa portions, with the greatest abundance in the IVA (Fig. 1C–F). The separation of a nerve fiber from the nerve bundle in ICB was abundant in one data stack (Fig. 1F), but scarce in the other two data stacks. These nerve fibers were separated from nerve bundles and running alone in the lamina propria (Fig. 1G). Enteric glial cells enwrapped the nerve fibers and were constantly found as a part of the nerve bundles (Fig. 1G); therefore, they were observed as different cells from the other cells in the lamina propria.

**Table 1.** The number of cells contacted with nerve fibers

| Class | Cell type | Contact no. | | | | |
|---|---|---|---|---|---|---|
| | | IVA | IVB | ICL | ICB | Total |
| FBLC | type I | 0 | 0 | 0 | 0 | 0 |
| | type II | 0 | 0 | 0 | 6 (4) | 6 (4) |
| | type III | 34 (14) | 4 (2) | 0 | 0 | 38 (16) |
| | type IV | 13 (8) | 2 (1) | 0 | 0 | 15 (9) |
| Immunocompetent cell | MLC | 18 (12) | 4 (1) | 0 | 2 (1) | 24 (14) |
| | Mono | 0 | 0 | 0 | 1 (1) | 1 (1) |
| | Plasma cell | 0 | 5 (0) | 0 | 0 | 5 (0) |
| | Eosinophil | 6 (3) | 0 | 0 | 0 | 6 (3) |
| | Mast cell | 0 | 2 (0) | 0 | 0 | 2 (0) |
| | Lym | 2 (1) | 2 (1) | 0 | 0 | 4 (2) |
| Epithelial cell | Paneth cell | 0 | 0 | 0 | 1 (1) | 1 (1) |
| | C-EC | 2 (0) | 0 | 0 | 0 | 2 (0) |
| | Goblet cell | 0 | 0 | 0 | 0 | 0 |
| | Endo | 0 | 0 | 0 | 0 | 0 |
| Others | VM | 0 | 1 (0) | 3 (0) | 1 (0) | 5 (0) |
| | Pericyte | 0 | 0 | 0 | 0 | 0 |
| | U.D. | 1 (1) | 2 (0) | 0 | 1 (1) | 4 (2) |
| Total | | 76 (39) | 22 (5) | 3 (0) | 12 (8) | 113 (52) |

C-EC, columnar epithelial cell; Endo, endocrine cell; FBLC, fibroblast-like cell; ICB, the basal portion of the crypts; ICL, the lateral portion of crypts; IVA, the apical portion of the villi; IVB, the basal portion of the villi; Lym, lymphocyte-like cell; MLC, macrophage-like cell; Mono, monocyte-like cell; U.D., undetermined cell; VM, villous myocyte. Numbers in parentheses are the numbers of digging structures. The fields are colored based on the contact number as follows. 0–4: gray, 5–9: pale red,10–: red.

*Analysis of the connectivity of nerve fibers in the rat ileal mucosa*

A total of 113 cells that were in contact with nerve fibers were detected (Table 1, Fig. 2). We previously reported the results of a qualitative analysis of the contacts of nerve fibers with type II–IV FBLCs [25]. The contact cells detected in the mucosa were abundant in the order of the IVA (n=76), IVB (n=22), ICB (n=12), and ICL (n=3) (Table 1). Nerve fibers were more frequently in contact with type III FBLCs, type IV FBLCs, and MLCs compared to the other cell types (Table 1). The contacts of nerve fibers with type II FBLCs (Fig. 2A) were restricted to the ICB, whereas the contacts with type III FBLCs (Fig. 2B) and type IV FBLCs (Fig. 2C) were observed mostly in the IVA.

Nerve fibers were also in contact with various types of cells including granulocytes such as eosinophils and mast cells and immunocompetent cells such as MLCs, a monocyte-like cell, plasma cells, and lymphocyte-like cells. Contacts with MLCs (Fig. 2D) were more frequently observed in the IVA compared to the other portions, although MLCs were sufficiently located in all portions. Only one monocyte-like cell was observed as a contact target of a nerve fiber in the ICB (Fig. 2E). Contacts with plasma cells (Fig. 2F) and mast cells (Fig. 2G) were observed only in the IVB, whereas those with eosinophils (Fig. 2H) were observed only in the IVA. Lymphocyte-like cells were scarcely in contact with the nerve fibers in the IVA and IVB (Fig. 2I). In addition, nerve bundles were running close to villous myocytes from the ICB to the IVA, although the direct contacts of nerve fibers with villous myocytes were scarce in all of the portions (Fig. 2J). Interestingly, only villous myocytes were in contact with the nerve fibers in the ICL.

Nerve fibers almost always ran more inside of lamina propria than subepithelial FBLCs, and thus contacts with epithelial cells were very scarce. The nerve fibers were in contact with only two villous columnar epithelial cells (Fig. 2K) and a Paneth cell (Fig. 2L), despite the basal surface of numerous epithelial cells contained in the data stacks was examined carefully. The one villous columnar epithelial cell and one Paneth cell extended a cellular process that penetrated the epithelial basement membrane toward the lamina propria, and these cells were in contact with the nerve fiber by their cellular process (Fig. 2K, 2L), whereas another villous columnar epithelial cell was in contact with a nerve fiber penetrating the epithelial basement membrane. Synaptic vesicle-like structures were usually observed in the nerve fibers at almost all contact sites (Fig. 2M). The nerve fibers at contact sites were occasionally digging into the cellular bodies of the target cells, especially type II FBLCs (Fig. 2A'), type III FBLCs (Fig. 2B'), type IV FBLCs (Fig. 2C'), MLCs (Fig. 2D'), eosinophils (Fig. 2H'), and lymphocyte-like cells (Fig. 2I') (as shown by the numbers in parentheses in Table 1), whereas these diggings of nerve fibers were not observed in the contact sites to plasma cells, mast cells, villous columnar epithelial cells, the Paneth cell, or villous myocytes.

We reconstructed the three-dimensional contact structures for each target cell type listed in Table 1. We observed that although some contact structures could not be three-dimensionally reconstructed, the other contact structures could be broadly classified into two patterns based on the number of nerve fibers contacting the target cells at one site: contact by a sole nerve fiber (sole-contact type: n=131), and contact by multiple nerve fibers (multi-contact type: n=39) (the total number of contact structure (n=170, Table 2)

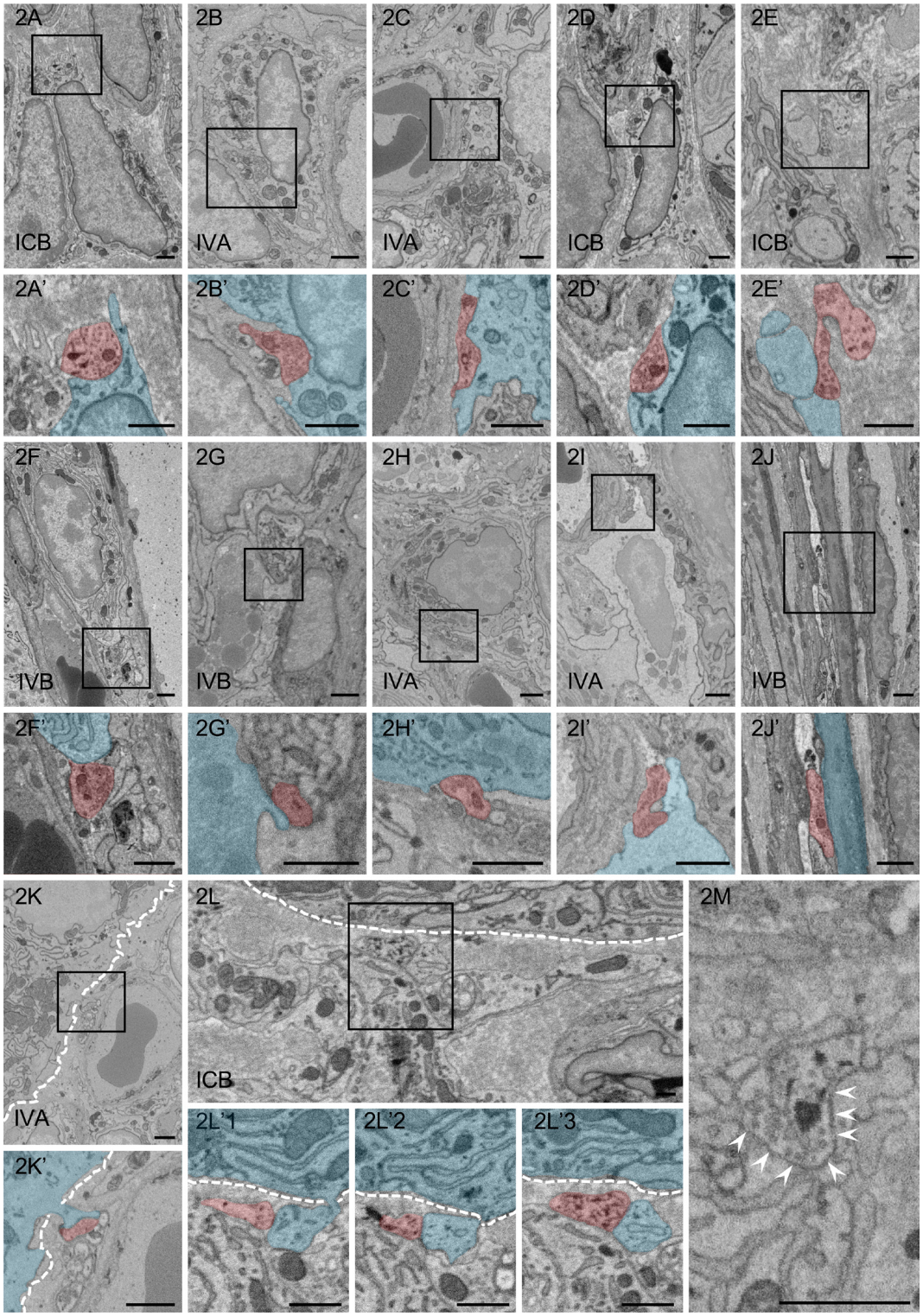


**Fig. 2.** Ultrastructural observation of contacts between nerve fibers (*red*) and target cells (*blue*). A–L: Nerve fibers are in contact with the type II fibroblast-like cell (FBLC) (A), the type III FBLC (B), the type IV FBLC (C), the macrophage-like cell (MLC) (D), the monocyte-like cell (E), the plasma cell (F), the mast cell (G), the eosinophil (H), the lymphocyte-like cell (I), the villous myocyte (J), the villous columnar epithelial cell (K), and the Paneth cell (L). A'–K': High-magnification images of the *squares* in panels A–K, respectively. Synaptic vesicle-like structures are observed in each contact structure. Contact structures against the type II FBLCs (A'), the type III FBLC (B'), the type IV FBLC (C'), the MLC (D'), the monocyte-like cell (E') the eosinophil (H') and the lymphocyte-like cell (I') dig into the cellular bodies of the target cells. L'1–3: Ultrastructural serial images showing the contact between a nerve fiber and a cellular process of the Paneth cell in panel L. L'3: High-magnification image from the *square* in panel L. The Paneth cell (*blue*) extends a cellular process penetrating the basal lamina and is in contact with a nerve fiber (*red*). M: Many synaptic vesicle-like structures are present in the contact structure showing the swelling pattern. A contact site between a nerve fiber and the type IV FBLC is indicated by *arrowheads* from the side of the type IV FBLC. *White dashed line*, epithelial basal lamina. IVA, apical portion of the villi. IVB, basal portion of the villi. ICB, basal portion of the crypts. Bar=1 $\mu$m.

**Table 2.** The number of contact structures in each pattern

| Pattern | Contact | Max. dia. | Relationship with NB | IVA | IVB | ICL | ICB | Total |
|---|---|---|---|---|---|---|---|---|
| #S1 | 1 | ≥1 $\mu$m | Separating | 14 | 1 | 0 | 9 | 24 |
| #S2 | 1 | ≥1 $\mu$m | Protruding | 50 | 11 | 1 | 2 | 64 |
| #S3 | 1 | <1 $\mu$m | Separating | 16 | 1 | 0 | 7 | 24 |
| #S4 | 1 | <1 $\mu$m | Protruding | 17 | 1 | 1 | 0 | 19 |
| #M | ≥2 | NA | Protruding | 27 | 11 | 1 | 0 | 39 |
| Total | | | | 124 | 25 | 3 | 18 | 170 |

#M, multi-contact type; NA, not applicable; NB, nerve bundle. The other abbreviations are explained in the Table 1 footnote.

was larger than the total number of contact cells (n=113, Table 1) because there were cases that two or more contact structures were observed against one target cell at the different sites). The maximum diameter of the nerve fibers at the contact structures of the sole-contact type was 0.332–3.118 $\mu$m, indicating that the contact structures included swelling patterns (>1 $\mu$m, 88/131) and non-swelling patterns (<1 $\mu$m, 43/131) (Fig. 3A). The nerve fibers of the sole-contact type were often in contact with each target cell without separating from nerve bundles (hereinafter referred to as the "protruding pattern", 83/131), whereas nerve fibers were occasionally in contact with each cell as a sole fiber that had completely separated from the nerve bundle (hereinafter referred to as the "separating pattern", 48/131). Therefore, the contact structures of the sole-contact type could be mainly classified into four patterns (#S1–#S4) based on both (1) the relationship with the nerve bundles (separating or protruding) and (2) the maximum diameter at the contact structures in the nerve fibers (swelling or non-swelling) as shown by Fig. 3B–F and Table 2.

Among the sole-contact type, pattern #S2 (protruding and swelling) was the most frequent, whereas pattern #S4 (protruding and non-swelling) was the least frequent. Pattern #S1 (separating and swelling) and #S3 (separating and non-swelling) showed similar numbers in the intermediate level between the pattern #S2 and #S4 (Table 2). The protruding patterns (#S2 and #S4, in total 83/131) were more abundant than the separating patterns (#S1 and #S3, in total 48/131) from the IVA to the ICL, whereas the separating patterns (#S1 and #S3) were more abundant than the protruding patterns in the ICB (Table 2). The contact structures sometimes dug into the cellular bodies of target cells in the swelling patterns (#S1 and #S2) but rarely did so in the non-swelling patterns (#S3 and #S4) (as described below in Table 3). Twelve cases among the swelling patterns (#S1 and #S2) showed that the distinctive contact structures branched slightly from the nerve fibers like a spine of dendrites in the brain (Fig. 3B).

In addition to the sole-contact type described above, we observed contact structures showing a multi-contact type in which each target cell was in contact with multiple (≥2) nerve fibers protruding from one nerve bundle (Fig. 3F–I), which means that the substantial contact number of the multi-contact type shown in Table 2 was less than that of the sole-contact type (Fig. 3G). This contact type increased toward IVA (Table 2). The contact structure of each nerve fiber in the multi-contact type usually corresponded to either of the protruding patterns #S2 or #S4 of the sole-contact type. Abundant digging structures by the many nerve fibers from one nerve bundle were observed against one target cell (Fig. 3H, 3I).

We recounted the numbers of nerve fiber-contacts against each cell type based on the above patterns shown in Fig. 3F (Table 3). Separating patterns (#S1 and/or #S3) were in contact with type II–IV FBLCs, MLCs, a mast cell, a Paneth cell, an eosinophil, a lymphocyte-like cell, and a monocyte-like cell. Pattern #S1 was often digging against type II–IV FBLCs and MLCs, whereas digging by pattern #S3 was highly scarce (as shown by the numbers in parentheses in Table 3). Pattern #S2 was in contact with many cell types other than monocyte-like cells, mast cells, lymphocytes-like cells and a Paneth cell, and this pattern showed digging against type III–IV FBLCs, MLCs, and an eosinophil. Pattern #S4 was in contact with type III–IV FBLCs, MLCs, a lymphocyte-like cell, a mast cell, a villous myocyte, and villous columnar epithelial cells and exhibited digging against only type III FBLCs. Moreover, the multi-contact type was in contact with type III–IV FBLCs, MLCs, plasma cells, eosinophils, lymphocytes-like cells, and villous myocytes. The multi-contact type exhibited at least one or more digging against the target cells other than plasma cells and villous myocytes, which was remarkable in type III FBLCs and MLCs. Interestingly, a large contact area by many nerve fibers against type III FBLCs was observed in this pattern, because a nerve bundle ran in a close position with type III FBLCs over a long distance (Fig. 3H, 3I).

All contact types (including both the sole-contact and multi-contact types) against most cell types (other than plasma cells, mast cells, a Paneth cell, and type II FBLCs) were abundant in the IVA, whereas in the ICB the target cells which were the most frequently in contact with pattern #S1 were type II FBLCs.

## DISCUSSION

Several studies have suggested that nerve fibers establish direct contacts with various types of cells in the small intestine [9, 16]. Direct contacts of nerve fibers with type II–IV FBLCs were also demonstrated by SBF-SEM in our previous study [25]. However, the contact structures of nerve fibers had been poorly defined, and the comprehensive targets of innervation had not been elucidated. Our present findings revealed that nerve fibers formed several patterns of contact structures containing synaptic vesicle-like structures against various types of cells in the rat ileal mucosa. Among them, the contact structures showing swelling patterns (#S1 and #S2; 1–3 $\mu$m)—which presumably correspond to the varicosity reported in earlier studies [12, 42]—often dug

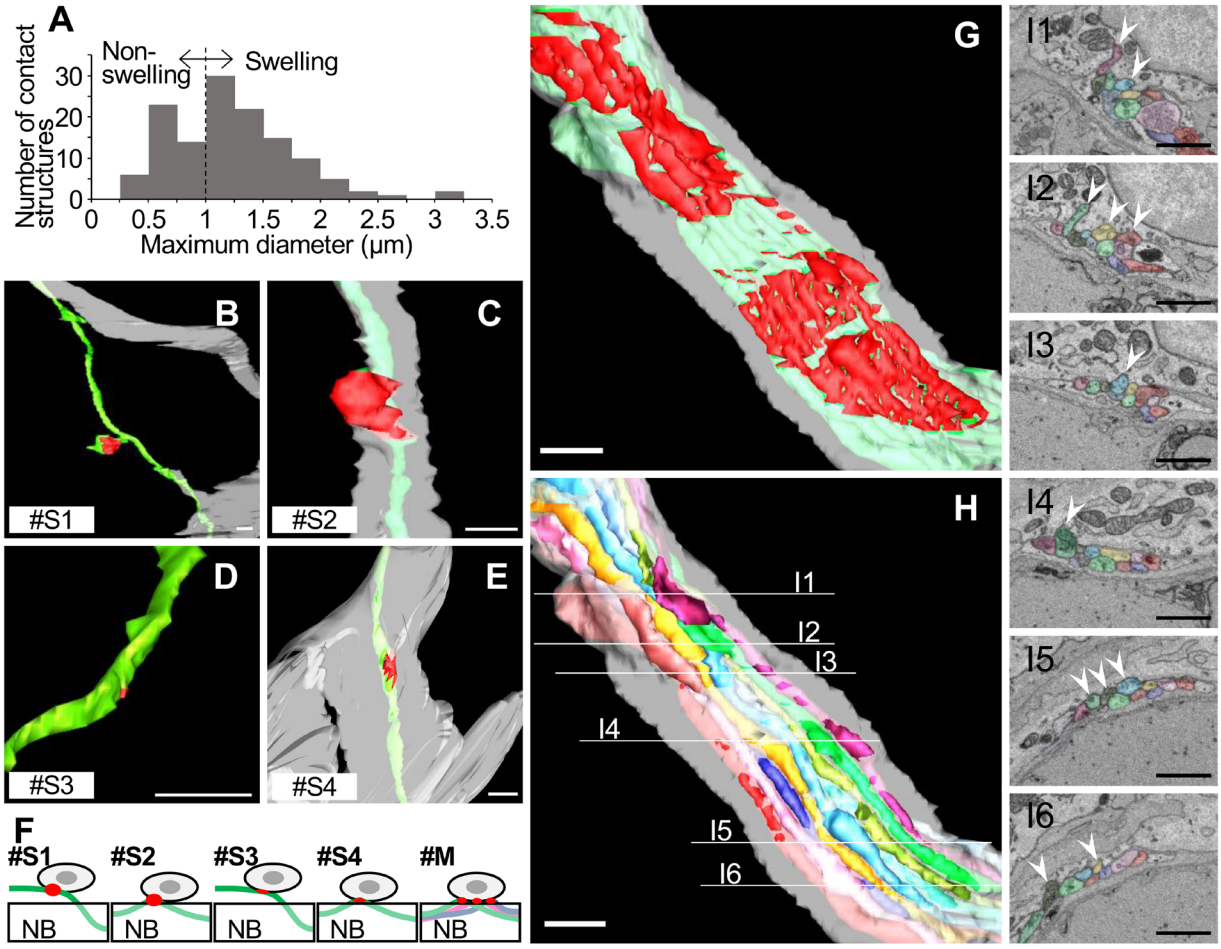


**Fig. 3.** Classification of contact structures based on 3D characteristics. A: The distribution of the maximum diameter of contact structures showing the sole-contact type. B–E: 3D images of contact structures in patterns #S1 (B), #S2 (C), #S3 (D), and #S4 (E). Contact-nerve fibers (*green*) separate from nerve bundles (*light gray*) in separating patterns (#S1, B; and #S3, D), while the nerve fibers other than those with contact sites are included in nerve bundles in protruding patterns (#S2, C; and #S4, E). The contact structure in panel B is branched slightly from the nerve fiber like a spine of dendrites in the brain (*arrow*). *Red*, contact site. Bar=1 $\mu$m. F: Schema of each pattern of contact structure. *Gray:* Target cell. *Red:* Contact structure. *Green*, *blue* and *pink:* Nerve fibers. NB: nerve bundle. #M: multi-contact type. G: 3D images of contact structures showing the multi-contact type. The multi-contact type has many contact sites (*red areas*) and collectively shows a large contact area. *Green:* Nerve fibers with contact structures. *Light gray:* Nerve bundle. H, I: 3D images of contact structures showing the multi-contact type (H) and ultrastructural serial images showing the contact between nerve fibers (colored in panel H) and their target cell (type III fibroblast-like cell (FBLC)) in the villous apical portion (I). The nerve bundle in panel H is the same as that in panel G. Each ultrastructural serial image in panel 3I represents the cross-sectional image shown in panel H. Multiple nerve fibers (each nerve fiber is shown by a different color) are contained in the same nerve bundle (*light gray*). Contact with type III FBLCs and digging into the cellular body (*white arrowheads*). The color of each nerve fiber in panel I corresponds to the color in panel H. G–I: Bar=1 $\mu$m.

into the target cells, suggesting that nerve fibers preferentially contact the target cells with directionality as swelling structures. The neurotransmission in the peripheral autonomic nervous system is thought to be mediated by varicosity [21], which is a swelling structure found in the middle of nerve fibers. It has also been reported that synaptic contact structures form swelling structures, including axonal endings and varicosities in the brain [22]. These studies suggest that swelling structures are one of the indexes of innervation, and thus the contact structures that we observed with (1) a swelling pattern (#S1 and #S2) and (2) digging into target cellular bodies (listed in Table 3 by the numbers in parentheses) suggest the existence of innervation with direct contacts in the rat ileal mucosa. We were unable to reach a conclusion regarding whether or not these contact structures include the synapse. In the case that we consider the above perspectives in the assessment of innervation (swelling and digging), it appears that type II–IV FBLCs, MLCs and eosinophils are all targets of innervation as listed in the parentheses in Table 3, although we cannot exclude the possibility that the other patterns of the contact structures also truly innervate target cells via direct contacts. In addition, the connective targets were portion-specific in the ileal mucosa: the contacts with type III–IV FBLCs, MLCs, and eosinophils were more abundant in the IVA, and those in contact with type II FBLCs were restricted to the ICB. Taken together, our results suggest that nerve fibers regulate the different functions or different cell types in each portion of the mucosa in the rat small intestine. The

**Table 3.** The number of contact patterns for each cell type in the four portions of the rat ileal mucosa

| Class | Cell type | Contact no. | | | | | | | | | | | | | | | | | | | | Total |
|---|---|---|---|---|---|---|---|---|---|---|---|---|---|---|---|---|---|---|---|---|---|---|
| | | IVA | | | | | IVB | | | | | ICL | | | | | ICB | | | | | |
| | | #S1 | #S2 | #S3 | #S4 | #M | #S1 | #S2 | #S3 | #S4 | #M | #S1 | #S2 | #S3 | #S4 | #M | #S1 | #S2 | #S3 | #S4 | #M | |
| FBLC | type II | 0 | 0 | 0 | 0 | 0 | 0 | 0 | 0 | 0 | 0 | 0 | 0 | 0 | 0 | 0 | 6 (4) | 2 (0) | 4 (0) | 0 | 0 | 12 (4) |
| | type III | 6 (2) | 13 (6) | 9 (1) | 10 (4) | 12 (6) | 0 | 3 (1) | 0 | 0 | 2 (1) | 0 | 0 | 0 | 0 | 0 | 0 | 0 | 0 | 0 | 0 | 55 (21) |
| | type IV | 3 (2) | 9 (6) | 2 (0) | 2 (0) | 4 (3) | 0 | 2 (1) | 0 | 0 | 1 (0) | 0 | 0 | 0 | 0 | 0 | 0 | 0 | 0 | 0 | 0 | 23 (12) |
| Imm | MLC | 5 (3) | 24 (12) | 3 (0) | 2 (0) | 6 (4) | 0 | 1 (0) | 0 | 0 | 3 (1) | 0 | 0 | 0 | 0 | 0 | 1 (1) | 0 | 1 (0) | 0 | 0 | 46 (21) |
| | Mono | 0 | 0 | 0 | 0 | 0 | 0 | 0 | 0 | 0 | 0 | 0 | 0 | 0 | 0 | 0 | 0 | 0 | 1 (1) | 0 | 0 | 1 (1) |
| | Plasma | 0 | 0 | 0 | 0 | 0 | 0 | 3 (0) | 0 | 0 | 2 (0) | 0 | 0 | 0 | 0 | 0 | 0 | 0 | 0 | 0 | 0 | 5 (0) |
| | Eosino | 0 | 3 (1) | 1 (0) | 0 | 3 (2) | 0 | 0 | 0 | 0 | 0 | 0 | 0 | 0 | 0 | 0 | 0 | 0 | 0 | 0 | 0 | 7 (3) |
| | Mast | 0 | 0 | 0 | 0 | 0 | 1 (0) | 0 | 0 | 1 (0) | 0 | 0 | 0 | 0 | 0 | 0 | 0 | 0 | 0 | 0 | 0 | 2 (0) |
| | Lym | 0 | 0 | 0 | 1 (0) | 2 (1) | 0 | 0 | 1 (1) | 0 | 2 (1) | 0 | 0 | 0 | 0 | 0 | 0 | 0 | 0 | 0 | 0 | 6 (3) |
| Epi | C-EC | 0 | 0 | 0 | 2 (0) | 0 | 0 | 0 | 0 | 0 | 0 | 0 | 0 | 0 | 0 | 0 | 0 | 0 | 0 | 0 | 0 | 2 (0) |
| | Paneth | 0 | 0 | 0 | 0 | 0 | 0 | 0 | 0 | 0 | 0 | 0 | 0 | 0 | 0 | 0 | 1 (0) | 0 | 0 | 0 | 0 | 1 (0) |
| Others | VM | 0 | 0 | 0 | 0 | 0 | 0 | 0 | 0 | 0 | 1 (0) | 0 | 1 (0) | 0 | 1 (0) | 1 (0) | 0 | 0 | 1 (0) | 0 | 0 | 5 (0) |
| | U.D. | 0 | 1 (1) | 1 (0) | 0 | 0 | 0 | 2 (0) | 0 | 0 | 0 | 0 | 0 | 0 | 0 | 0 | 1 (1) | 0 | 0 | 0 | 0 | 5 (2) |

Eosino, eosinophil; Epi, epithelial cell; Imm, immunocompetent cell; Mast, mast cell; Paneth, Paneth cell. The other abbreviations are same as Tables 1 and 2 footnote. Numbers in parentheses are the numbers of digging structures. The fields are colored based on the contact number as follows. 0–4: gray, 5–9: pale red, 10–: red.

possible significance of contacts by nerve fibers with each type of cell is discussed next.

Subepithelial FBLCs (type III in this study) in the rat small intestine form a mesh-like structure under the epithelium [25] and communicate with each other by gap junctions [9, 14]. These cells were reported to be in contact with various other cells (e.g., villous myocytes and nerve fibers) by cellular processes. FBLCs and villous myocytes are thought to support the villous structure and contracting of the intestinal villi [9, 14]. Subepithelial and non-subepithelial FBLCs are in contact with villous myocytes by cellular processes, suggesting that these cells might act together as a contraction system [19, 25]. It has been pointed out the possibility that the pumping motion of the intestinal villi may cause the flow of lymph in the central lacteal [23]. These findings provide a foundation for the hypothesis that the contraction system formed by villous FBLCs and villous myocytes might regulate pumping of the intestinal villi to promote the flow of lymph in the central lacteal from the top toward the bottom of the intestinal villus. In the present study, abundant neural connections with subepithelial FBLCs (type III) and non-subepithelial FBLCs (type IV) were observed in the IVA. This finding suggests that type III FBLCs and type IV FBLCs are subject to many innervations, especially in the IVA, which might lead to the efficient flowing of lymph in the central lacteal from the top to the base by pumping. The tissue structure in the IVA is thought to be susceptible to physical stimulation by the luminal contents and to be prone to deformation of the intestinal villi. This information about physical stimulation is speculated to be received by subepithelial FBLCs (type III FBLCs in this study) and transmitted to the nervous system by intrinsic primary afferent neurons (IPANs) [13] which have dendrites that also function as axons and are in contact with subepithelial FBLCs [2]. We observed herein that the contact structures against type III FBLCs were the most abundant, especially in the IVA, and included the multi-contact type in which many nerve fibers were in contact with and dug into the cellular bodies of type III FBLCs, which means that multiple nerve fibers could simultaneously regulate one individual type III FBLC. These findings suggest that type III FBLCs in the IVA might actively attract nerve fibers via unknown mechanisms and be delicately regulated by various nerve fibers including IPANs; this presumably contributes to the well-known functions of type III FBLCs, which include receiving physical stimulations [13] and collaboratively contracting [16].

The mucosal epithelium in the intestinal crypt has been reported to be affected by various neurotransmitters. For example, ACh and VIP increase the secretion of intestinal juice [1, 37], and CGRP and SP upregulate the proliferation of epithelial cells in the rat intestine [17]. ACh promotes the secretion of antibacterial substances in Paneth cells [35]. Despite these reports about the functional effects of neurotransmitters on epithelial cells in the intestinal crypt, evidence of the innervation with direct contact to the epithelial cells other than tuft cells and endocrine cells [28, 41] had been never presented. In our present investigation, the nerve fibers almost always ran in the lamina propria more inside than the subepithelial FBLCs and were not in contact with crypt epithelial cells (except for a Paneth cell). It is not yet clear whether the contacts of nerve fibers with a Paneth cell were true innervation, because the contact structure was neither swelling nor digging. These results provide the following alternative hypothesis that the major innervation pathway to the crypt epithelial cells occurs without direct contact: (1) the nerve fibers innervate the crypt epithelial cells by paracrine-manner (without direct contact) or (2) any of cells in the lamina propria mediate the neurotransmission to the crypt epithelium. In this study, the main targets of neural connections around the intestinal crypt were the type II FBLCs. Our earlier investigation revealed that type II FBLCs form a basket-like reticular structure surrounding the crypt epithelium by being in contact with each other around the intestinal crypts [25]. Such FBLCs around the crypts were immunopositive for CD34 and in direct contact with Paneth cells [26]. Therefore, considering that the secretion of antibacterial

substances from Paneth cells is promoted by ACh [35] despite scarce direct contacts as shown in the present study, we speculate that type II FBLCs might regulate the secretion of antibacterial substances, and possibly intestinal juice, by mediating neurotransmission to crypt epithelial cells. The basket-like reticular structure formed by type II FBLCs surrounding the intestinal crypt might contribute to efficient signal transduction from nerve fibers to the wide range of crypt epithelial cells by acting as a "spreader", in contrast to the direct regulation of epithelial cells by each neuron. On the other hand, although the connect between the epithelial cells and nerve fibers were highly scarce in the present study, the extensions of the cellular process from epithelial cells into the lamina propria found in the present study might be noteworthy. This phenomenon has been reported in Paneth cells [26] and intestinal enteroendocrine cells [3]. The extension of the cellular processes penetrating the basal lamina might be important for intercellular communication between the epithelial cells and the cells in the lamina propria. The data stacks used in the present study will be helpful to quantify this phenomenon. It is required to more detailed investigation about that in the future to clarify its significance.

The activation of macrophages has been reported to be regulated by ACh [40]. Vagotomy, knockdown of the vesicular ACh transporter, and administration of an ACh-antagonist promoted the phagocytosis of macrophages (Kupffer cells) in the mouse liver [10]. In addition, inflammatory activity is inhibited by ACh through the nicotinic ACh receptor of peritoneal macrophages from mice [5]. The ENS has been suggested to control inflammation by innervating macrophages through a cholinergic anti-inflammatory pathway [27]. VIP also inhibit the inflammatory activities of macrophages, such as inhibition of TNFα synthesis [7] and upregulation of IL-10 synthesis [6]. Moreover, mononuclear phagocytes in the mouse ileum express VIP receptor (VPAC1) and are in contact with $VIP^+$ nerve fibers [4]. Thus, neural contributions to the regulation of the functions of macrophage have become well known, but the precise picture of innervation against macrophages is poorly understood. Our present analyses suggest that MLCs were the second most abundantly innervated cell type after type III FBLCs and that MLCs were in contact with nerve fibers mainly in the IVA, although MLCs existed in all portions of the mucosa. These findings suggest that nerve fibers preferentially innervate MLCs in IVA compared to the other types of immunocompetent cells and might contribute to the maintenance of intestinal homeostasis by regulating their fundamental functions (e.g., phagocytosis and cytokine production). However, considering that macrophages contribute to the reconstruction of the neural network in the brain [36] and the myenteric plexus in the intestine [24], we cannot exclude the possibility that the contacts between nerve fibers and macrophages might contain the neural connection for the maintenance or the reconstruction of the enteric neural network in the intestinal mucosa as well as innervation. To investigate these two hypotheses, it is necessary to examine the significance of contacts between nerve fibers and MLCs in further studies. We identified not only MLCs but also eosinophils as the candidate targets of innervation in this study. These findings suggest that the nerve fibers may control various immune functions in the intestinal mucosa.

ACKNOWLEDGMENTS. The Ketjen black was kindly provided by Dr. N. Ohno (Jichi Medical University). This study was financially supported by the Japan Society for the Promotion of Science (grant no. 16K18813 and 20K15902).

## REFERENCES

1. Barbezat, G. O. and Grossman, M. I. 1971. Intestinal secretion: stimulation by peptides. *Science* **174**: 422–424. [Medline] [CrossRef]
2. Bertrand, P. P., Kunze, W. A., Bornstein, J. C. and Furness, J. B. 1998. Electrical mapping of the projections of intrinsic primary afferent neurones to the mucosa of the guinea-pig small intestine. *Neurogastroenterol. Motil.* **10**: 533–541. [Medline] [CrossRef]
3. Bohórquez, D. V., Samsa, L. A., Roholt, A., Medicetty, S., Chandra, R. and Liddle, R. A. 2014. An enteroendocrine cell-enteric glia connection revealed by 3D electron microscopy. *PLoS One* **9**: e89881. [Medline] [CrossRef]
4. Buckinx, R., Alpaerts, K., Pintelon, I., Cools, N., Van Nassauw, L., Adriaensen, D. and Timmermans, J. P. 2017. In situ proximity of CX3CR1-positive mononuclear phagocytes and VIP-ergic nerve fibers suggests VIP-ergic immunomodulation in the mouse ileum. *Cell Tissue Res.* **368**: 459–467. [Medline] [CrossRef]
5. de Jonge, W. J., van der Zanden, E. P., The, F. O., Bijlsma, M. F., van Westerloo, D. J., Bennink, R. J., Berthoud, H. R., Uematsu, S., Akira, S., van den Wijngaard, R. M. and Boeckxstaens, G. E. 2005. Stimulation of the vagus nerve attenuates macrophage activation by activating the Jak2-STAT3 signaling pathway. *Nat. Immunol.* **6**: 844–851. [Medline] [CrossRef]
6. Delgado, M., Munoz-Elias, E. J., Gomariz, R. P. and Ganea, D. 1999*a*. Vasoactive intestinal peptide and pituitary adenylate cyclase-activating polypeptide enhance IL-10 production by murine macrophages: *in vitro* and *in vivo* studies. *J. Immunol.* **162**: 1707–1716. [Medline]
7. Delgado, M., Pozo, D., Martinez, C., Leceta, J., Calvo, J. R., Ganea, D. and Gomariz, R. P. 1999*b*. Vasoactive intestinal peptide and pituitary adenylate cyclase-activating polypeptide inhibit endotoxin-induced TNF-alpha production by macrophages: *in vitro* and *in vivo* studies. *J. Immunol.* **162**: 2358–2367. [Medline]
8. Denk, W. and Horstmann, H. 2004. Serial block-face scanning electron microscopy to reconstruct three-dimensional tissue nanostructure. *PLoS Biol.* **2**: e329. [Medline] [CrossRef]
9. Desaki, J., Fujiwara, T. and Komuro, T. 1984. A cellular reticulum of fibroblast-like cells in the rat intestine: scanning and transmission electron microscopy. *Arch. Histol. Jpn.* **47**: 179–186. [Medline] [CrossRef]
10. Fonseca, R. C., Bassi, G. S., Brito, C. C., Rosa, L. B., David, B. A., Araújo, A. M., Nóbrega, N., Diniz, A. B., Jesus, I. C. G., Barcelos, L. S., Fontes, M. A. P., Bonaventura, D., Kanashiro, A., Cunha, T. M., Guatimosim, S., Cardoso, V. N., Fernandes, S. O. A., Menezes, G. B., de Lartigue, G. and Oliveira, A. G. 2019. Vagus nerve regulates the phagocytic and secretory activity of resident macrophages in the liver. *Brain Behav. Immun.* **81**: 444–454. [Medline] [CrossRef]
11. Furness, J. B. 2012. The enteric nervous system and neurogastroenterology. *Nat. Rev. Gastroenterol. Hepatol.* **9**: 286–294. [Medline] [CrossRef]
12. Furuya, S. and Furuya, K. 2007. Subepithelial fibroblasts in intestinal villi: roles in intercellular communication. *Int. Rev. Cytol.* **264**: 165–223. [Medline] [CrossRef]
13. Furuya, S. and Furuya, K. 2013. Roles of substance P and ATP in the subepithelial fibroblasts of rat intestinal villi. *Int. Rev. Cell Mol. Biol.* **304**:

133–189. [Medline] [CrossRef]
14. Furuya, S., Furuya, K., Sokabe, M., Hiroe, T. and Ozaki, T. 2005. Characteristics of cultured subepithelial fibroblasts in the rat small intestine. II. Localization and functional analysis of endothelin receptors and cell-shape-independent gap junction permeability. *Cell Tissue Res.* **319**: 103–119. [Medline] [CrossRef]
15. Gallacher, M., Mackenna, B. R. and McKirdy, H. C. 1973. Effects of drugs and of electrical stimulation on the muscularis mucosae of rabbit large intestine. *Br. J. Pharmacol.* **47**: 760–764. [Medline] [CrossRef]
16. Güldner, F. H., Wolff, J. R. and Keyserlingk, D. G. 1972. Fibroblasts as a part of the contractile system in duodenal villi of rat. *Z. Zellforsch. Mikrosk. Anat.* **135**: 349–360. [Medline] [CrossRef]
17. Hoffmann, P., Mazurkiewicz, J., Holtmann, G., Gerken, G., Eysselein, V. E. and Goebell, H. 2002. Capsaicin-sensitive nerve fibres induce epithelial cell proliferation, inflammatory cell immigration and transforming growth factor-alpha expression in the rat colonic mucosa *in vivo*. *Scand. J. Gastroenterol.* **37**: 414–422. [Medline] [CrossRef]
18. Holzer, P. and Guth, P. H. 1991. Neuropeptide control of rat gastric mucosal blood flow. Increase by calcitonin gene-related peptide and vasoactive intestinal polypeptide, but not substance P and neurokinin A. *Circ. Res.* **68**: 100–105. [Medline] [CrossRef]
19. Hosoyamada, Y. and Sakai, T. 2007. Mechanical components of rat intestinal villi as revealed by ultrastructural analysis with special reference to the axial smooth muscle cells in the villi. *Arch. Histol. Cytol.* **70**: 107–116. [Medline] [CrossRef]
20. Iwanaga, T., Hoshi, O., Han, H., Takahashi-Iwanaga, H., Uchiyama, Y. and Fujita, T. 1994. Lamina propria macrophages involved in cell death (apoptosis) of enterocytes in the small intestine of rats. *Arch. Histol. Cytol.* **57**: 267–276. [Medline] [CrossRef]
21. Kandel, E. R., Schwartz, J. H. and Jessel, T. M. 2000. Principles of neural science, 4th ed., McGraw-Hill, New York.
22. Kasthuri, N., Hayworth, K. J., Berger, D. R., Schalek, R. L., Conchello, J. A., Knowles-Barley, S., Lee, D., Vázquez-Reina, A., Kaynig, V., Jones, T. R., Roberts, M., Morgan, J. L., Tapia, J. C., Seung, H. S., Roncal, W. G., Vogelstein, J. T., Burns, R., Sussman, D. L., Priebe, C. E., Pfister, H. and Lichtman, J. W. 2015. Saturated reconstruction of a volume of neocortex. *Cell* **162**: 648–661. [Medline] [CrossRef]
23. Kokas, E. 1965. Intestinal villous motility and its regulation. *Am. J. Dig. Dis.* **10**: 974–976. [Medline] [CrossRef]
24. Kulkarni, S., Micci, M. A., Leser, J., Shin, C., Tang, S. C., Fu, Y. Y., Liu, L., Li, Q., Saha, M., Li, C., Enikolopov, G., Becker, L., Rakhilin, N., Anderson, M., Shen, X., Dong, X., Butte, M. J., Song, H., Southard-Smith, E. M., Kapur, R. P., Bogunovic, M. and Pasricha, P. J. 2017. Adult enteric nervous system in health is maintained by a dynamic balance between neuronal apoptosis and neurogenesis. *Proc. Natl. Acad. Sci. USA* **114**: E3709–E3718. [Medline] [CrossRef]
25. Mantani, Y., Haruta, T., Nishida, M., Yokoyama, T., Hoshi, N. and Kitagawa, H. 2019. Three-dimensional analysis of fibroblast-like cells in the lamina propria of the rat ileum using serial block-face scanning electron microscopy. *J. Vet. Med. Sci.* **81**: 454–465. [Medline] [CrossRef]
26. Mantani, Y., Nishida, M., Yamamoto, K., Miyamoto, K., Yuasa, H., Masuda, N., Omotehara, T., Tsuruta, H., Yokoyama, T., Hoshi, N. and Kitagawa, H. 2018. Ultrastructural and immunohistochemical study on the lamina propria cells beneath Paneth cells in the rat ileum. *Anat. Rec. (Hoboken)* **301**: 1074–1085. [Medline] [CrossRef]
27. Matteoli, G., Gomez-Pinilla, P. J., Nemethova, A., Di Giovangiulio, M., Cailotto, C., van Bree, S. H., Michel, K., Tracey, K. J., Schemann, M., Boesmans, W., Vanden Berghe, P. and Boeckxstaens, G. E. 2014. A distinct vagal anti-inflammatory pathway modulates intestinal muscularis resident macrophages independent of the spleen. *Gut* **63**: 938–948. [Medline] [CrossRef]
28. Morroni, M., Cangiotti, A. M. and Cinti, S. 2007. Brush cells in the human duodenojejunal junction: an ultrastructural study. *J. Anat.* **211**: 125–131. [Medline] [CrossRef]
29. Nagahama, M., Semba, R., Tsuzuki, M. and Ozaki, T. 2001. Distribution of peripheral nerve terminals in the small and large intestine of congenital aganglionosis rats (Hirschsprung's disease rats). *Pathol. Int.* **51**: 145–157. [Medline] [CrossRef]
30. Neild, T. O., Shen, K. Z. and Surprenant, A. 1990. Vasodilatation of arterioles by acetylcholine released from single neurones in the guinea-pig submucosal plexus. *J. Physiol.* **420**: 247–265. [Medline] [CrossRef]
31. Nguyen, H. B., Thai, T. Q., Saitoh, S., Wu, B., Saitoh, Y., Shimo, S., Fujitani, H., Otobe, H. and Ohno, N. 2016. Conductive resins improve charging and resolution of acquired images in electron microscopic volume imaging. *Sci. Rep.* **6**: 23721. [Medline] [CrossRef]
32. Ohno, N., Katoh, M., Saitoh, Y., Saitoh, S. and Ohno, S. 2015. Three-dimensional volume imaging with electron microscopy toward connectome. *Microscopy (Oxf.)* **64**: 17–26. [Medline] [CrossRef]
33. Piper, P. J., Said, S. I. and Vane, J. R. 1970. Effects on smooth muscle preparations of unidentified vasoactiv peptides from intestine and lung. *Nature* **225**: 1144–1146. [Medline] [CrossRef]
34. Qu, Z. D., Thacker, M., Castelucci, P., Bagyánszki, M., Epstein, M. L. and Furness, J. B. 2008. Immunohistochemical analysis of neuron types in the mouse small intestine. *Cell Tissue Res.* **334**: 147–161. [Medline] [CrossRef]
35. Satoh, Y. 1988. Atropine inhibits the degranulation of Paneth cells in ex-germ-free mice. *Cell Tissue Res.* **253**: 397–402. [Medline] [CrossRef]
36. Schafer, D. P., Lehrman, E. K., Kautzman, A. G., Koyama, R., Mardinly, A. R., Yamasaki, R., Ransohoff, R. M., Greenberg, M. E., Barres, B. A. and Stevens, B. 2012. Microglia sculpt postnatal neural circuits in an activity and complement-dependent manner. *Neuron* **74**: 691–705. [Medline] [CrossRef]
37. Sidhu, M. and Cooke, H. J. 1995. Role for 5-HT and ACh in submucosal reflexes mediating colonic secretion. *Am. J. Physiol.* **269**: G346–G351. [Medline]
38. Stead, R. H., Tomioka, M., Quinonez, G., Simon, G. T., Felten, S. Y. and Bienenstock, J. 1987. Intestinal mucosal mast cells in normal and nematode-infected rat intestines are in intimate contact with peptidergic nerves. *Proc. Natl. Acad. Sci. USA* **84**: 2975–2979. [Medline] [CrossRef]
39. Timmermans, J. P., Hens, J. and Adriaensen, D. 2001. Outer submucous plexus: an intrinsic nerve network involved in both secretory and motility processes in the intestine of large mammals and humans. *Anat. Rec.* **262**: 71–78. [Medline] [CrossRef]
40. Van Der Zanden, E. P., Boeckxstaens, G. E. and de Jonge, W. J. 2009. The vagus nerve as a modulator of intestinal inflammation. *Neurogastroenterol. Motil.* **21**: 6–17. [Medline] [CrossRef]
41. Wade, P. R. and Westfall, J. A. 1985. Ultrastructure of enterochromaffin cells and associated neural and vascular elements in the mouse duodenum. *Cell Tissue Res.* **241**: 557–563. [Medline] [CrossRef]
42. Wang, X. Y., Sanders, K. M. and Ward, S. M. 1999. Intimate relationship between interstitial cells of cajal and enteric nerves in the guinea-pig small intestine. *Cell Tissue Res.* **295**: 247–256. [Medline] [CrossRef]